LONGITUDINAL LOSS OF LANDAU DAMPING IN DOUBLE HARMONIC RF SYSTEMS BELOW TRANSITION ENERGY

L. Intelisano*,[1], H. Damerau, I. Karpov, CERN, Geneva, Switzerland
[1]also at Sapienza Università di Roma, Rome, Italy

Abstract

Landau damping plays a crucial role in ensuring single-bunch stability in hadron synchrotrons. In the longitudinal plane, loss of Landau damping (LLD) occurs when a coherent mode of oscillation moves out of the incoherent synchrotron frequency band. The LLD threshold is studied for a purely inductive impedance below transition energy, specifically considering the common case of double harmonic RF systems operating in counter-phase at the bunch position. The additional focusing force due to beam-induced voltage distorts the potential well, ultimately collapsing the bucket. The limiting conditions for a binomial particle distribution are calculated. Furthermore, the contribution focuses on the configuration of the higher-harmonic RF system at four times the fundamental RF frequency operating in phase. In this case, the LLD threshold shows a non-monotonic behavior with a zero threshold where the derivative of the synchrotron frequency distribution is positive. The findings are obtained employing semi-analytical calculations using the MELODY code.

INTRODUCTION

In the longitudinal plane, Landau damping [1] is established by the synchrotron frequency spread of individual particles caused by the non-linear voltage of the RF system [2–14]. A common technique to enhance beam stability is employing multiple RF systems, which can enlarge the synchrotron frequency spread.

This work focuses on the common case of a double-harmonic RF (DRF) system and considers a pure inductive impedance below the transition energy or, equivalently, capacitive impedance above it.

DRF systems are based on employing a higher harmonic RF system, typically working at a multiple of the fundamental RF frequency. In this configuration, the total voltage experienced by the particles is given by

$$V_{\mathrm{rf}}(\phi) = V_0[\sin(\phi+\phi_{s0}) + r\sin(n\phi + n\phi_{s0} + \Phi_2)]\,, \quad (1)$$

where V_0, r, and ϕ_{s0} are the voltage magnitudes of the main harmonic RF system, the voltage ratio between the higher and the fundamental harmonic number, and the phase of the synchronous particle. As far as ϕ, n, and Φ_2 are concerned, they represent the phase offset with respect to the synchronous particle, the harmonic number ratio, and the relative phase between the two RF systems. Two distinct operational modes can be distinguished depending on the relative phase Φ_2. Bunch shortening mode (BSM) occurs when the RF systems are in phase at the bunch position, leading to shorter bunches. On the contrary, when the RF systems are in counter-phase, it is referred to as bunch lengthening mode (BLM). Figure 1 illustrates the synchrotron frequency distributions for different orders of RF harmonic number ratio, n, in both configurations.

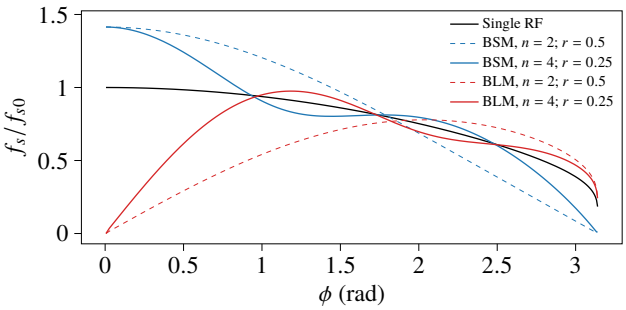

Figure 1: Synchrotron frequency distribution, normalized to small-amplitude synchrotron frequency, f_{s0}, in a single-harmonic RF system (black), BSM (blue) and BLM (red), as a function of the maximum phase deviation of the particle. No acceleration and collective effects are considered.

The studies presented in this contribution have been conducted with semi-analytical calculations using the code MELODY [15], based on the Oide-Yokya method [16]. To allow a direct comparison with the analysis for single RF [12] and BSM above transition [17], the same accelerator parameters outlined in Table 1 have been considered.

Table 1: Main RF Parameters of the LHC

Parameter	Unit	Value
Circumference, $2\pi R$	m	26658.86
Main harmonic number, h		35640
Main RF frequency, f_{rf}	MHz	400.79
Beam energy at injection, E_0	TeV	0.45
Main RF voltage V_0	MV	6
Effective impedance, $\mathrm{Im}Z/k$	Ω	−0.07

MAIN EQUATIONS AND DEFINITIONS

For convenience, the analysis is performed with the set of variables $(\mathcal{E},\psi)$ to describe the longitudinal beam dynamics, which correspond to the energy and phase of the synchrotron oscillations:

$$\mathcal{E} = \frac{\dot{\phi}^2}{2\omega_{s0}^2} + U_t(\phi)\,,$$
$$\psi = \mathrm{sgn}(\eta\Delta E)\frac{\omega_s(\mathcal{E})}{\sqrt{2}\omega_{s0}}\int_{\phi_{\max}}^{\phi}\frac{\mathrm{d}\phi'}{\sqrt{\mathcal{E}-U_t(\phi')}}\,, \quad (2)$$

* leandro.intelisano@cern.ch

where ΔE and ω_{s0} are the energy offset with respect to the synchronous particle and the angular frequency of small amplitude synchrotron oscillations in a single RF, $\eta = 1/\gamma_{tr}^2 - 1/\gamma^2$ is the phase slip factor, and γ_{tr} is the Lorentz factor at transition energy.

The solution for the stationary potential U_t, in Eq. (2), can be obtained by using an iterative procedure [11], with given step m, as follows

$$\begin{aligned} U_{t,m} &= (1-\epsilon)U_{t,m-1} + \epsilon U_t\left(\lambda_{m-1}\right); \\ U_{t,m} &= U_{t,m} - \min\left(U_{t,m}\right); \\ \lambda_m &= \lambda\left(U_{t,m}\right); m = 1, 2, \ldots . \end{aligned} \tag{3}$$

If it exists, the solution to this system of equations can be found for small convergence parameter $\epsilon > 0$.

Hereafter, only particle distributions belonging to a binomial family will be considered, i. e.

$$g(\mathcal{E}) = \left(1 - \frac{\mathcal{E}}{\mathcal{E}_{\max}}\right)^{\mu}, \tag{4}$$

where, depending on μ, it covers most of the realistic bunch distributions in proton synchrotrons, from flat ($\mu = -1/2$) to Gaussian ($\mu \to \infty$). The corresponding line density is

$$\lambda(\phi) = \lambda_0 \left[1 - \frac{U_t(\phi)}{\mathcal{E}_{\max}}\right]^{\mu+1/2}, \tag{5}$$

where the normalization

$$\int_{-\phi_{\max}}^{\phi_{\max}} \lambda(\phi) \mathrm{d}\phi = 1, \tag{6}$$

has been imposed.

UPPER LIMIT INTENSITY DUE TO POTENTIAL WELL DISTORTION

In the case of constant inductive impedance and taking into account binomial distribution according to Eq. (4), the total steady-state potential in Eq. (3) can be written in an implicit form, as follows [5]:

$$U_t(\phi) = U_{\mathrm{rf}}(\phi) + \zeta \mathrm{Im}Z/k \left[\lambda(\phi) - \lambda_0\right], \tag{7}$$

where $\mathrm{Im}Z/k$=const, k represents the revolution harmonic, and ζ is the intensity parameters defined

$$\zeta = \frac{2\pi q N_p h^2 f_0}{V_0}, \tag{8}$$

with f_0 as the revolution frequency.

Note that $U_t(\phi_{\max}) = \mathcal{E}_{\max}$, where $\mathcal{E}_{\max}$ and $\phi_{\max}$ are respectively the maxima of the synchrotron oscillation energy and phase of the total potential in the bunch. Assuming $\mu = 0.5$ one gets

$$U_{\mathrm{rf}}(\phi_{\max}) = \mathcal{E}_{\max} + \zeta\lambda_0 . \tag{9}$$

Substituting Eq. (9) into Eq. (7), the total potential can then be written

$$U_t(\phi) = U_{\mathrm{rf}}(\phi) \frac{\mathcal{E}_{\max}}{U_{\mathrm{rf}}(\phi_{\max})} . \tag{10}$$

Therefore, the total potential is directly proportional to the RF potential.

Inserting Eq. (10) into Eq. (5), we can integrate over the maximum phase to obtain λ_0:

$$\lambda_0 = \frac{1}{\int_{-\phi_{\max}}^{\phi_{\max}} \left(1 - \frac{U_{\mathrm{rf}}(\phi)}{U_{\mathrm{rf}}(\phi_{\max})}\right) \mathrm{d}\phi} . \tag{11}$$

Eventually, combining Eqs. (11) and (9), yields:

$$\zeta_{\mathrm{cc}} = \left(U_{\mathrm{rf}}(\phi_{\max}) - \mathcal{E}_{\max}\right) \int_{-\phi_{\max}}^{\phi_{\max}} \left(1 - \frac{U_{\mathrm{rf}}(\phi)}{U_{\mathrm{rf}}(\phi_{\max})}\right) \mathrm{d}\phi . \tag{12}$$

Equation (12) represents the critical intensity parameter. The induced voltage acts as a focusing force when $\eta \mathrm{Im}Z/k < 0$. Therefore, the total potential well shrinks with the intensity, ultimately collapsing the buckets. Results obtained by iterative procedure (Eq. (3)) confirm the analytic predictions given by Eq. (12) and are shown in Fig. 2. In the case of $\mu \neq 0.5$, only empirically fitted functions are proposed for the moment.

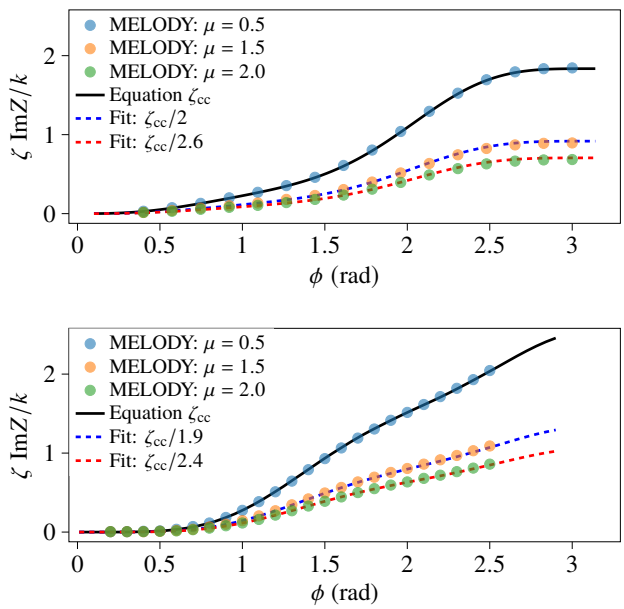

Figure 2: Comparison between the critical curve Eq. (12) (black) and MELODY (dots) in the BSM (top) and BLM (bottom) configurations is considered for harmonic and voltage ratios $n = 4$ and $r = 0.25$, respectively. For distribution functions with $\mu = 1.5$ and $\mu = 2.0$, fitted functions (dashed lines) are proposed.

LLD DAMPING BELOW TRANSITION ENERGY

For $\eta \mathrm{Im}Z/k < 0$, i. e., inductive impedance below transition energy (or capacitive above), coherent modes emerge

below the minimum incoherent frequency. Hence, LLD threshold is reached when $\Omega \equiv \min[\omega_s(\mathcal{E})]$. In configurations where the minimum falls on the tail of the frequency distribution, such as BSM (or BLM in specific cases), we expect that the LLD is independent of the cutoff frequency, as seen in single RF case [12].

Figure 3 summarizes the LLD threshold, computed using MELODY, as a function of the particle phase deviation in BSM. For a harmonic number ratio of $n = 2$, Fig. 3a confirms that the LLD threshold is independent of the cutoff frequency for $\mu = 1.5$ (diamonds) and in agreement with the single RF system case [12]. Furthermore, the threshold disappears beyond the critical curve for larger bunch lengths. Also for particle distributions with $\mu = 0.5$, this dependence persists.

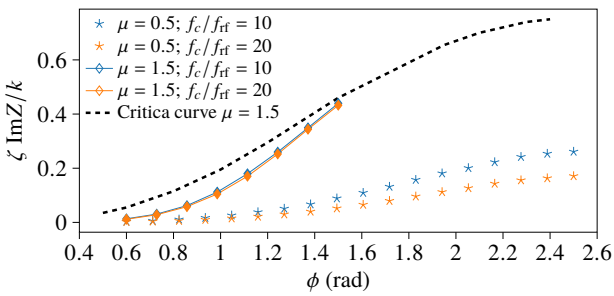

(a) $n = 2$; $r = 0.5$.

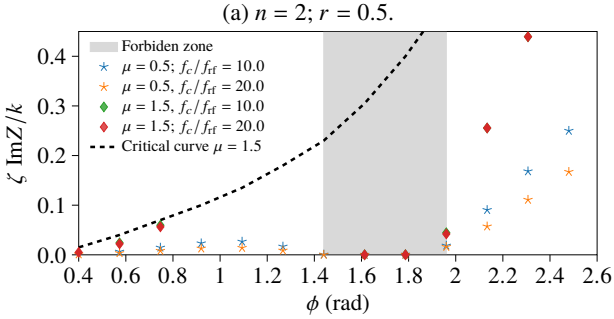

(b) $n = 4$; $r = 0.25$.

Figure 3: The LLD threshold, computed using MELODY, as a function of the maximum phase deviation of the particle in BSM. The second harmonic case (top) is illustrated for different cutoff frequencies, f_c. The fourth harmonic case is shown at the bottom for $\mu = 0.5$ and $\mu = 1.5$. A forbidden zone is highlighted in grey where $\mathrm{d}f_s/\mathrm{d}\phi > 0$.

In the fourth harmonic configuration, the LLD is no longer a monotonic function [17] caused by the presence of a positive derivative in the synchrotron frequency distribution. This grey zone where $\mathrm{d}f_s/\mathrm{d}\phi > 0$ [11] represents a region in which the LLD vanishes and coherent instabilities can easily be triggered. Similarly to the $n = 2$ case, dependence on the cutoff frequency is not observed for particle distribution with $\mu = 1.5$ (diamonds), while being present for $\mu = 0.5$. Moreover, the LLD threshold exceeds the critical curve around $\phi = 0.8$ rad.

In BLM, Fig. 4 shows that the LLD threshold is monotonic with the maximum phase deviation of the particle, contrary to the case $\eta \mathrm{Im}Z/k > 0$ [9, 11, 13].

Note that in Fig. 4b, there are points with a jump of the derivative of the LLD threshold over the phase. This is linked to the fact that upon a certain bunch length, the minimum of the synchrotron frequency distribution moves from the center to the tail of the bunch and, hence, is no longer being dependent on the cutoff frequency, similar to the BSM case.

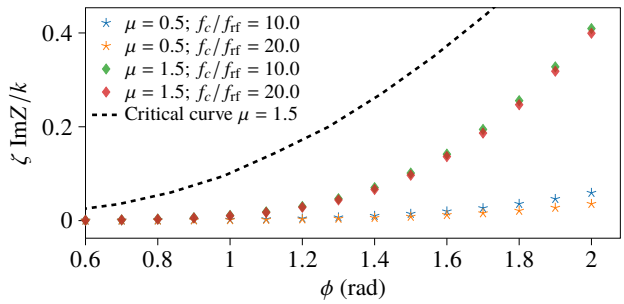

(a) $n = 2$; $r = 0.1$.

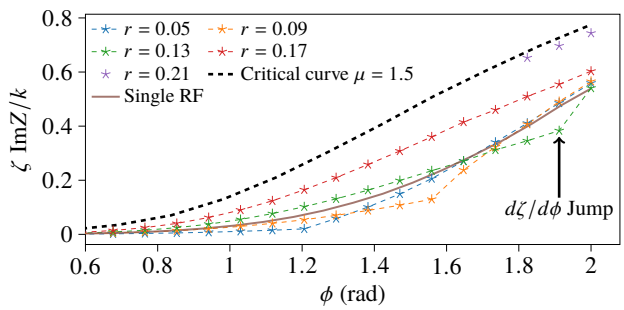

(b) $n = 4$; $\mu = 1.5$.

Figure 4: The LLD threshold in BLM computed semi-analytically with the MELODY code. The case of $n = 2$ is illustrated on the top for different distributions and cutoff frequencies. On the bottom, the fourth harmonic RF system, $n = 4$, is considered and compared with the single RF case (solid line). The black dashed line represents the critical curve for $\mu = 1.5$.

CONCLUSION

The loss of Landau damping in synchrotrons is a critical condition that can lead to beam instabilities and particle loss. The present study focuses on the LLD threshold within the common configuration of BSM and BLM when inductive impedances below transition energy (or capacitive above) are involved. The limiting intensity for a binomial particle distribution was calculated analytically and compared with results from the semi-analytical code MELODY.

In BSM, loss of dependency on the cutoff frequency in the LLD threshold agrees with the prediction showing a non-monotonic behavior. As expected, regions where $\mathrm{d}f_s/\mathrm{d}\phi > 0$ led to a vanishing LLD threshold at any intensity. On the contrary, in BLM, the LLD threshold results in a monotonic function.

REFERENCES

[1] L. D. Landau, "On the vibrations of the electronic plasma", *J. Phys.*, vol. 10, pp. 25–34, 1946.

[2] A. N. Lebedev, "Coherent synchrotron oscillations in the presence of a space charge", *Atomic Energy*, vol. 25, no. 2, pp. 851–856, 1968. doi:10.1007/BF01121037

[3] F. J. Sacherer, "A longitudinal stability criterion for bunched beams", *IEEE Trans. Nucl. Sci.*, vol. 20, pp. 825-829, 1973. doi:10.1109/TNS.1973.4327254

[4] F. J. Sacherer, "Methods for computing bunched-beam instabilities", CERN, Geneva, Switzerland, Rep. CERN-SI-INT-BR-72-5, 1972. https://cds.cern.ch/record/322545

[5] A. Hofmann and F. Pedersen, "Bunches with local elliptic energy distributions", *IEEE Trans. Nucl. Sci.*, vol. 26, pp. 3526–3528, 1979. doi:10.1109/TNS.1979.4330088

[6] G. Besnier, "Stabilité des oscillations longitudinales d'un faisceau groupe se propageant dans une chambre a vide d'impedance reactive", *Nucl. Instrum. Methods*, vol. 164, pp. 235–245, 1979. doi.org:10.1016/0029-554X(79)90241-6

[7] Y. H. Chin, K. Satoh, and K. Yokoya, "Instability of a bunched beam with synchrotron frequency spread", *Part. Accel.*, vol. 13, pp. 45–66, 1983. https://cds.cern.ch/record/140624

[8] V. I. Balbekov and S. V. Ivanov, "The Influence of Chamber Inductance on the Threshold of Longitudinal Bunched Beam Instability", in *Proc. EPAC'90*, Nice, France, Jun. 1990, pp. 1566–1569.

[9] O. Boine-Frankenheim and T. Shukla, "Space charge effects in bunches for different RF wave forms", *Phys. Rev. Spec. Top. Accel. Beams*, vol. 8, p. 034201, 2005. doi:10.1103/PhysRevSTAB.8.034201

[10] O. Boine-Frankenheim and O. Chorniy, "Stability of coherent synchrotron oscillations with space charge", *Phys. Rev. Spec. Top. Accel. Beams*, vol. 10, p. 104202, 2007. doi:10.1103/PhysRevSTAB.10.104202

[11] A. V. Burov, "Van Kampen Modes for Bunch Longitudinal Motion", in *Proc. HB'10*, Morschach, Switzerland, Sep.-Oct. 2010, pp. 358–362. https://jacow.org/HB2010/papers/TUO1C03.pdf

[12] I. Karpov, T. Argyropoulos, and E. Shaposhnikova, "Thresholds for loss of landau damping in longitudinal plane", *Phys. Rev. Accel. Beams*, vol. 24, p. 011002, 2021. doi:10.1103/PhysRevAccelBeams.24.011002

[13] L. Intelisano, H. Damerau and I. Karpov, "Measurements of longitudinal Loss of Landau damping in the CERN Proton Synchrotron", in *Proc. IPAC'23*, Venice, Italy, May 2023, pp. 2665–2668. doi:10.18429/JACoW-IPAC2023-WEPA012

[14] L. Intelisano, H. Damerau and I. Karpov, "Longitudinal loss of Landau damping in the CERN super proton synchrotron at 200 GeV", in *Proc. IPAC'23*, Venice, Italy, May 2023, pp. 2669–2672. doi:10.18429/JACoW-IPAC2023-WEPA013

[15] I. Karpov, "Matrix Equations for Longitudinal beam DYnamics (MELODY) code". https://gitlab.cern.ch/ikarpov/melody

[16] K. Oide and K. Yokoya, "Longitudinal single bunch instability in electron storage rings", KEK, Tsukuba, Japan, KEK-Preprint 90-10, 1990.

[17] L. Intelisano, H. Damerau, and I. Karpov, "Threshold for Loss of Longitudinal Landau Damping in Double Harmonic RF Systems", in *Proc. HB'21*, Batavia, IL, USA, Oct. 2021, pp. 95–99. doi:10.18429/JACoW-HB2021-MOP15

Temporary page!

LaTeX was unable to guess the total number of pages correctly. As there was some unprocessed data that should have been added to the final page this extra page has been added to receive it.

If you rerun the document (without altering it) this surplus page will go away, because LaTeX now knows how many pages to expect for this document.